

## Electronic Supplementary Information

# Dendrite-free and anticaustic Zn anode enabled by high current-induced reconstruction of electrical double layer

Yang-feng Cui,<sup>ab</sup> Ren-fei Cao,<sup>ab</sup> Jia-yi Du,<sup>b</sup> Zhen-bang Zhuang,<sup>b</sup> Zi-long Xie,<sup>b</sup> Qing-shuang Wang,<sup>d</sup> Di Bao,<sup>b</sup> Wan-qiang Liu,<sup>\*a</sup> Yun-hai Zhu,<sup>\*c</sup> and Gang Huang<sup>\*b</sup>

<sup>a</sup> School of Materials Science and Engineering, Changchun University of Science and Technology, Changchun 130022, China

<sup>b</sup> State Key Laboratory of Rare Earth Resource Utilization, Changchun Institute of Applied Chemistry, Chinese Academy of Sciences, Changchun 130022, China

<sup>c</sup> Research Center for Nanotechnology, Changchun University of Science and Technology, Changchun 130022, China.

<sup>d</sup> State Key Laboratory of New Textile Materials and Advanced Processing Technologies, Wuhan Textile University, Wuhan 430200, China

## Experimental Section

**Materials.** Zinc sulfate heptahydrate ( $\text{ZnSO}_4 \cdot 7\text{H}_2\text{O}$ , 99%), potassium sulphate ( $\text{K}_2\text{SO}_4$ , 99%) and commercial vanadium pentoxide ( $\text{V}_2\text{O}_5$ , 99%) were obtained from Sigma Aldrich. Zn foil (99.9%, 50  $\mu\text{m}$  thickness), Ti foil and carbon papers were obtained from the Canrd New Energy Technology. Graphite was purchased from Aladdin.

**Fabrication of  $\text{V}_2\text{O}_5$  electrode.** The commercial  $\text{V}_2\text{O}_5$  and graphite with a mass ratio of 8: 2 were filled into the ball-milling jar and their mixture was ball milled at 600 rpm for 360 min. Subsequently, the  $\text{V}_2\text{O}_5$  electrode was prepared by uniformly grinding the ball-milled  $\text{V}_2\text{O}_5$ /graphite mixture and polyvinylidene fluoride (PVDF) in a mass ration of 9: 1 in N-methyl-2-pyrrolidone (NMP) solvent. Finally, the mixture of ball-milled  $\text{V}_2\text{O}_5$ /graphite mixture/PVDF was coated on the carbon papers and dried in the vacuum oven at 80 °C for 24 h. The loading mass of active mass is  $\sim 5.0 \text{ g cm}^{-2}$ .

**Fabrication of the cells.** The Zn//Zn, Zn//Cu, and Zn// $\text{V}_2\text{O}_5$  batteries were assembled using CR2032 coin cells, aqueous 3 M  $\text{ZnSO}_4$  electrolyte and glass fibre separator (GF/A, Whatman).

**Materials characterization.** SEM was carried out with a field emission scanning electron microanalyser (Hitachi S4800). XRD patterns were collected on a Bruker D8 Focus powder X-ray diffractometer using Cu  $K\alpha$  radiation.

**Electrochemical measurements.** The Zn electrodeposits were obtained in a three-electrode system using the Commercial Zn of Ti foil as the working electrode, Ag/AgCl reference electrode and Zn foil as counter electrode. Line polarization curves were performed at a scan rate of 0.1  $\text{mV s}^{-1}$  in 3.0 M ZS electrolytes using the Zn deposit as working electrode, Ag/AgCl reference electrode and Pt mesh as counter electrode. Linear sweep voltammetry curves of Zn deposits were obtained in 0.5 M  $\text{K}_2\text{SO}_4$  electrolyte with a scan rate of 5.0  $\text{mV s}^{-1}$  using the Zn deposit as working electrode, Ag/AgCl reference electrode and Pt mesh as counter electrode. Zn electrodeposition, line polarization curves, and linear sweep voltammetry were carried out on a Biologic VMP3 system. The cell performances of Zn//Zn, Zn//Cu and Zn// $\text{V}_2\text{O}_5$  batteries using the galvanostatic method were performed in a Land instrument.

## Theoretical methods.

Molecular dynamics (MD) simulations were performed to investigate the distribution of aqueous 3.0 M ZS aqueous solution on Zn electrode surface. The four-layer electrode was composed of 1188 Zn atoms with dimensional sizes of 41.14  $\text{\AA} \times 40.09 \text{\AA} \times 6.50 \text{\AA}$ . The aqueous ZS solution had a dimension of 41.14  $\text{\AA} \times 40.09 \text{\AA} \times 50.0 \text{\AA}$ , which contained 148  $\text{Zn}^{2+}$ , 148  $\text{SO}_4^{2-}$ , and 2740  $\text{H}_2\text{O}$  placed on the electrode surface. The density of  $\text{ZnSO}_4$  solution in MD simulation is 1.48  $\text{g cm}^{-3}$  (corresponded to 3.0 M). Three different charged conditions for electrode were investigated, which were obtained from the simplified Grahame equation:<sup>1</sup>

$$\sigma = 0.117 \sinh(\psi_0/51.4) [\text{ZS}] \text{ C m}^{-2} \quad (1)$$

where the electrode surface charge density ( $\sigma$ ) can be calculated by the electrode surface

potential ( $\psi_0$ ) and the concentration of ZS ([ZS]). The electrode surface potentials were obtained from the symmetric Zn//Zn batteries, which are ca. 30, 50, and 75 mV at 1, 4, and 16 mA cm<sup>-2</sup>, respectively (Fig. 1a-c). Since the concentration of ZS is 3.0 M, the charge densities of electrode surface were calculated to -0.13, -0.23 and -0.41 C m<sup>-2</sup> at 1, 4, and 16 mA cm<sup>-2</sup>, respectively.

All MD simulations were carried out using the LAMMPS package.<sup>2</sup> The universal force field (UFF) was adopted to describe the bond and non-bond interactions.<sup>3</sup> Water molecule was described by the SPC/E model.<sup>4</sup> Van der Waals and Coulomb interactions were calculated using a cut-off value of 12.5 Å. Equations of motion were integrated by leapfrog algorithm with a time step of 1 fs. After energy minimization, each system was fully optimized under periodic boundary conditions for 2.0 ns in the NVT (T = 298 K) ensemble using the Nose-Hoover thermostat. After reaching equilibrium state, another 1.0 ns simulation was performed to output number density for Zn<sup>2+</sup> ions, SO<sub>4</sub><sup>2-</sup> ions, and H<sub>2</sub>O molecules, and radial distribution function (RDF) for SO<sub>4</sub><sup>2-</sup> ions and H<sub>2</sub>O molecules with respect to Zn<sup>2+</sup> ions.

## Reference

1. J. N. Israelachvili, *Intermolecular and Surface Forces*, 3rd ed.,; Elsevier: London, 2011.
2. S. Plimpton, *J. Comput. Phys.*, 1995, **117**, 1–19.
3. A. K. Rappe, C. J. Casewit, K. S. Colwell, W. A. Goddard, W. M. Skiff, W. M., Uff, *J. Am. Chem. Soc.*, 1992, **114**, 10024–10035.
4. H. J. C. Berendsen, J. R. Grigera, T. P. Straatsma, *J. Phys. Chem.*, 1987, 91, 6269–6271.

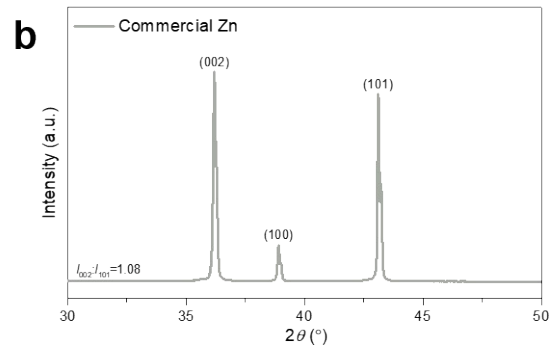
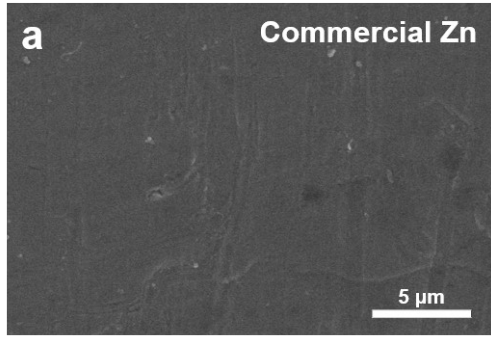


**Figure S1.** (a) SEM image of commercial Zn and (b) the corresponding XRD pattern.

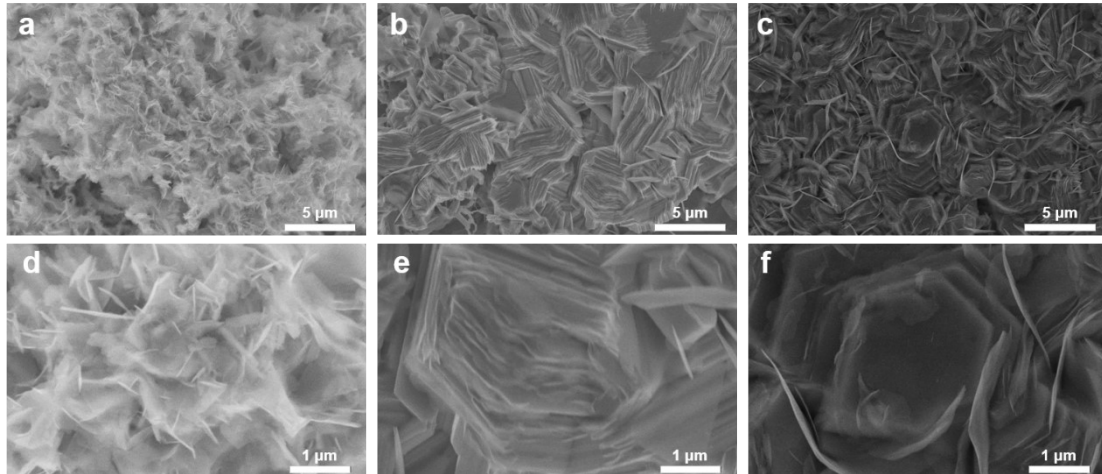


**Figure S2.** (a-f) SEM images of the plated Zn morphology on commercial Zn substrates in 0.5 M ZS electrolyte at (a, d) 1 mA cm<sup>-2</sup>, (b, e) 4 mA cm<sup>-2</sup>, and (c, f) 16 mA cm<sup>-2</sup> with a fixed plated areal capacity of 3 mAh cm<sup>-2</sup>.

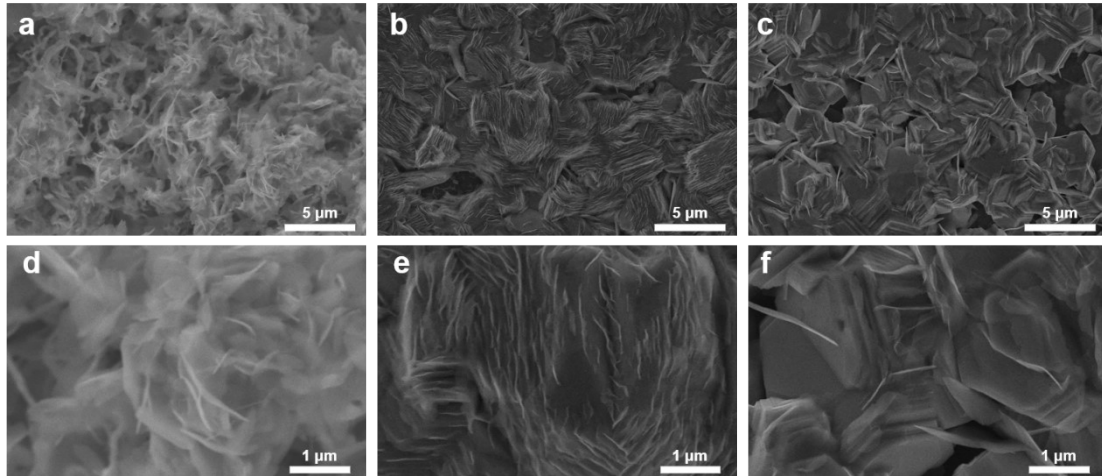


**Figure S3.** (a-f) SEM images of the plated Zn morphology on commercial Zn substrates in 1.0 M ZS electrolyte at (a, d) 1 mA cm<sup>-2</sup>, (b, e) 4 mA cm<sup>-2</sup>, and (c, f) 16 mA cm<sup>-2</sup> with a fixed plated areal capacity of 3 mAh cm<sup>-2</sup>.

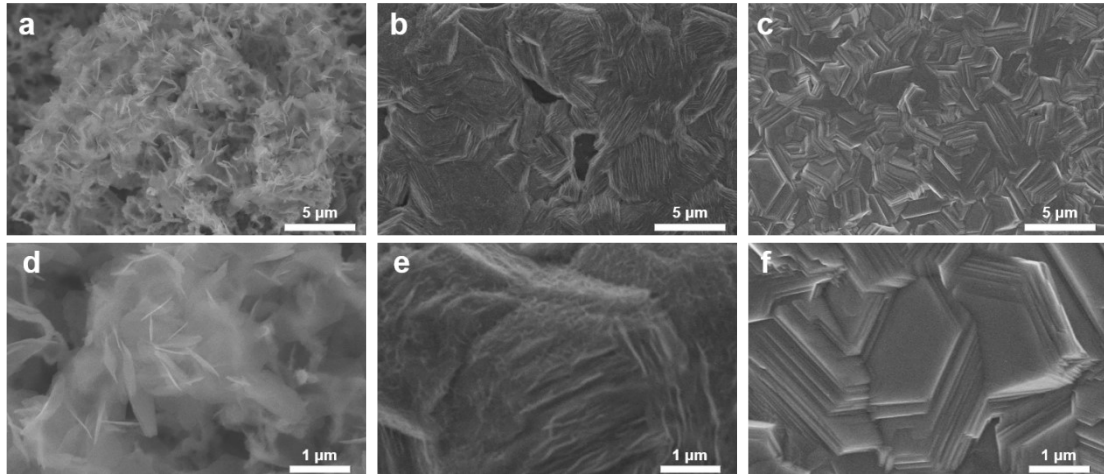


**Figure S4.** (a-f) SEM images of the plated Zn morphology on commercial Zn substrates in 2.0 M ZS electrolyte at (a, d) 1 mA cm<sup>-2</sup>, (b, e) 4 mA cm<sup>-2</sup>, and (c, f) 16 mA cm<sup>-2</sup> with a fixed plated areal capacity of 3 mAh cm<sup>-2</sup>.

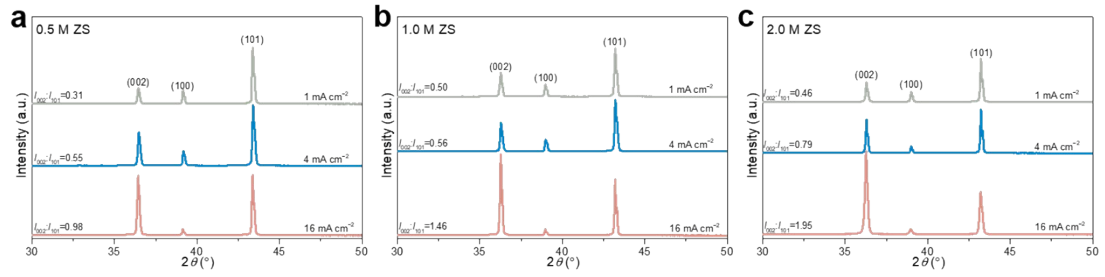


**Figure S5.** (a-c) XRD patterns of Zn electrodeposits in (a) 0.5 M ZS, (b) 1.0 M ZS, and (c) 2.0 M ZS electrolytes on Zn substrates at different current densities (1, 4, and 16  $\text{mA cm}^{-2}$ ) with a fixed areal capacity of 3  $\text{mAh cm}^{-2}$ .

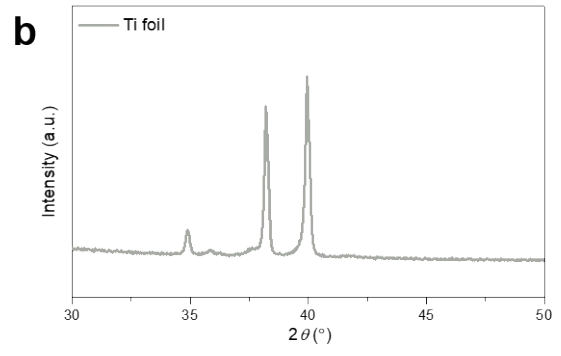
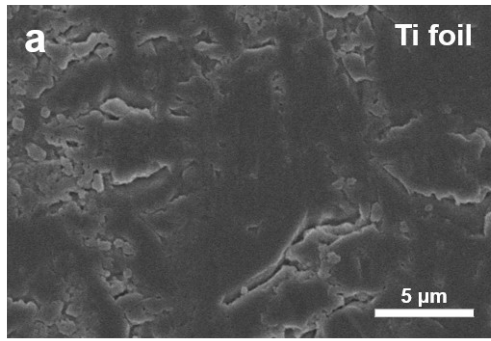


**Figure S6.** (a) SEM image of Ti foil and (b) the corresponding XRD pattern.

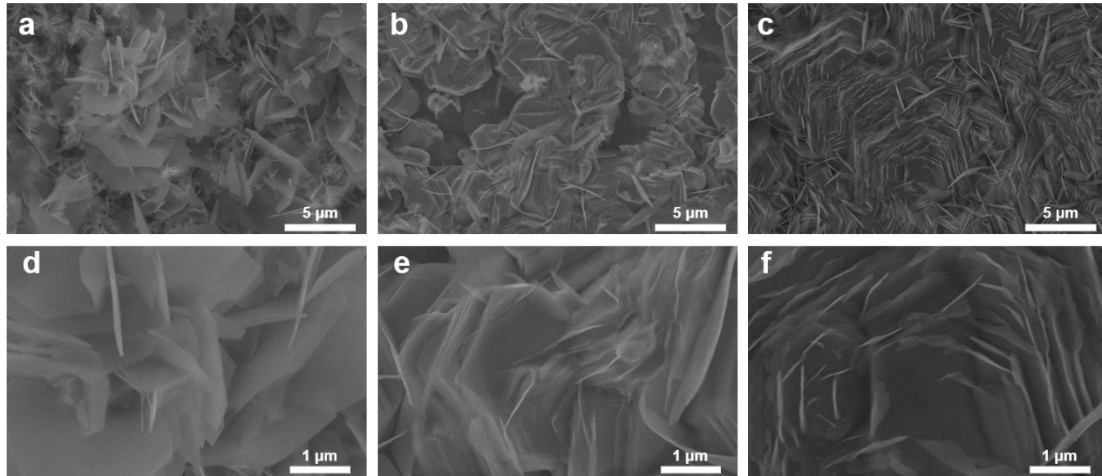


**Figure S7.** (a-f) SEM images of the plated Zn morphology on Ti substrates in 0.5 M ZS electrolyte at (a, d)  $1 \text{ mA cm}^{-2}$ , (b, e)  $4 \text{ mA cm}^{-2}$ , and (c, f)  $16 \text{ mA cm}^{-2}$  with a fixed areal capacity of  $3 \text{ mAh cm}^{-2}$ .

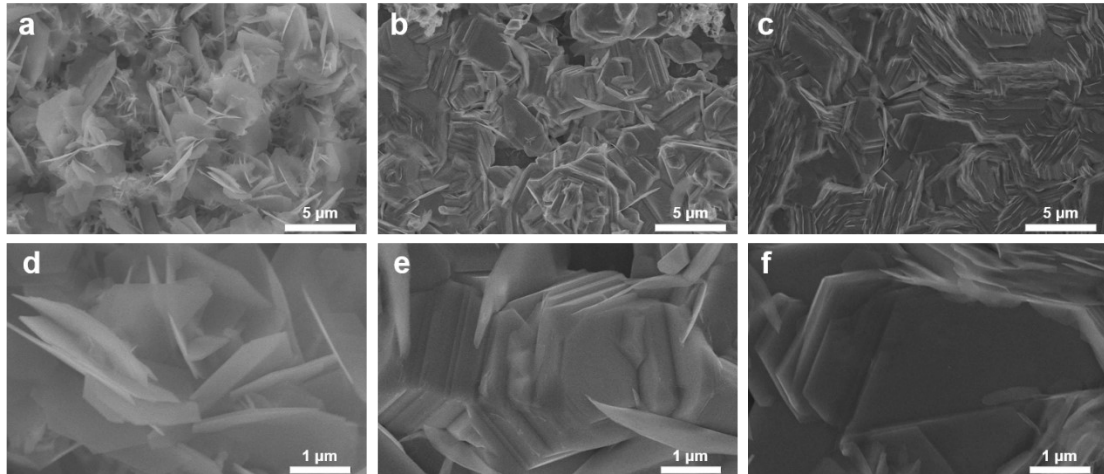


**Figure S8.** (a-f) SEM images of the plated Zn morphology on Ti substrates in 1.0 M ZS electrolyte at (a, d) 1 mA cm<sup>-2</sup>, (b, e) 4 mA cm<sup>-2</sup>, and (c, f) 16 mA cm<sup>-2</sup> with a fixed areal capacity of 3 mAh cm<sup>-2</sup>.

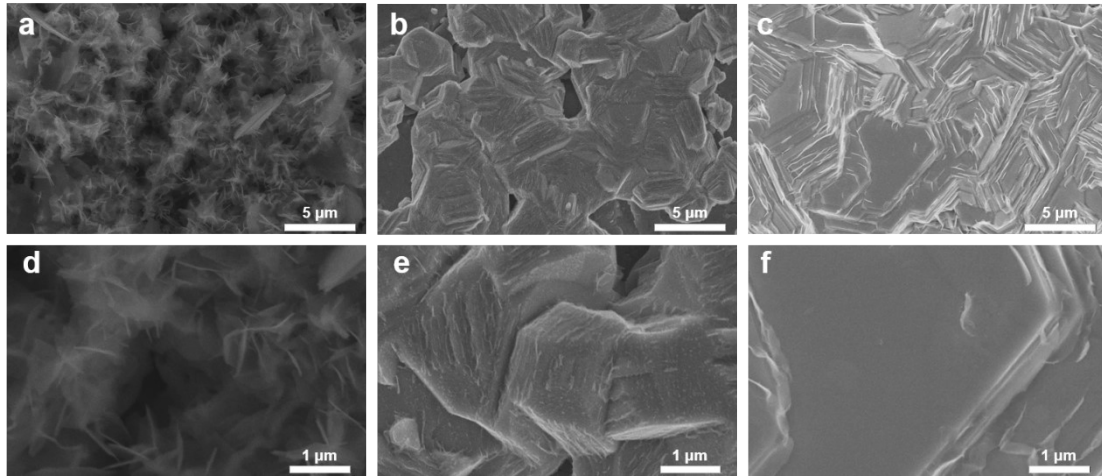


**Figure S9.** (a-f) SEM images of the plated Zn morphology on Ti substrates in 2.0 M ZS electrolyte at (a, d) 1 mA cm<sup>-2</sup>, (b, e) 4 mA cm<sup>-2</sup>, and (c, f) 16 mA cm<sup>-2</sup> with a fixed areal capacity of 3 mAh cm<sup>-2</sup>.

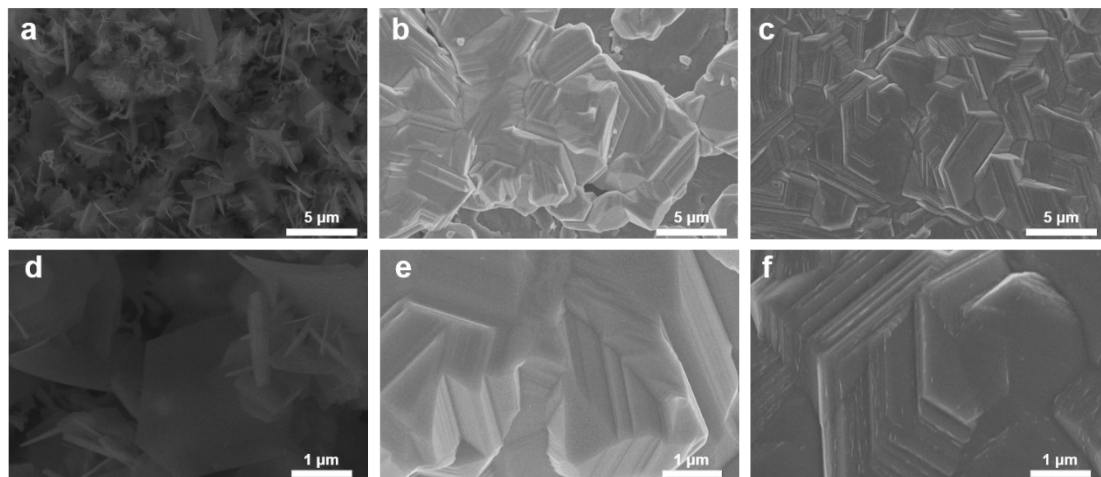


**Figure S10.** (a-f) SEM images of the plated Zn morphology on Ti substrates in 3.0 M ZS electrolyte at (a, d)  $1 \text{ mA cm}^{-2}$ , (b, e)  $4 \text{ mA cm}^{-2}$ , and (c, f)  $16 \text{ mA cm}^{-2}$  with a fixed areal capacity of  $3 \text{ mAh cm}^{-2}$ .

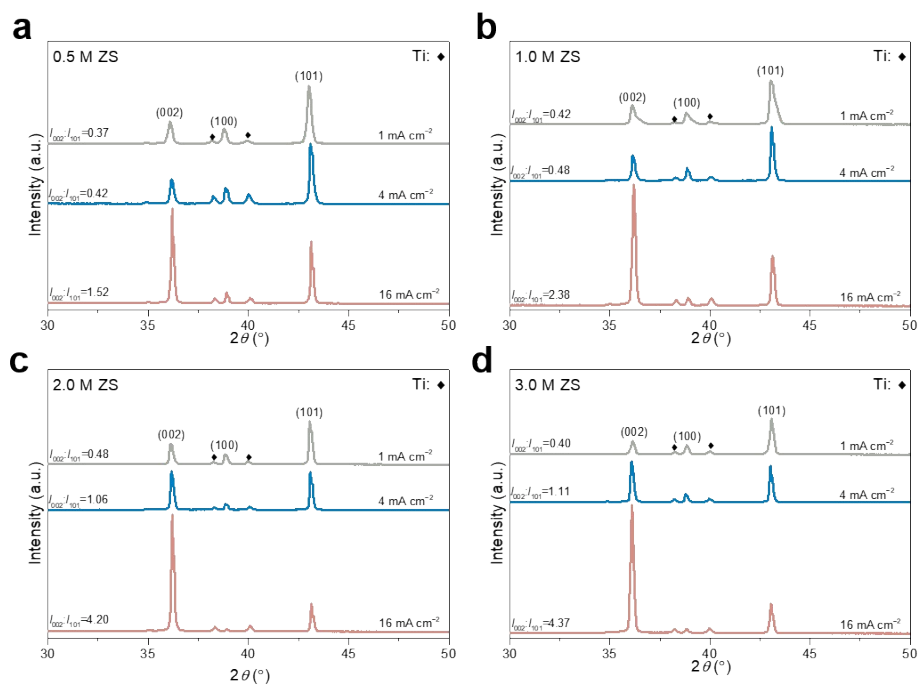


**Figure S11.** (a-d) XRD patterns of Zn electrodeposits in (a) 0.5 M ZS, (b) 1.0 M ZS, (c) 2.0 M ZS, and (d) 3.0 M ZS electrolytes on Ti substrates at different current densities (1, 4, and 16 mA cm<sup>-2</sup>) with a fixed areal capacity of 3 mAh cm<sup>-2</sup>.

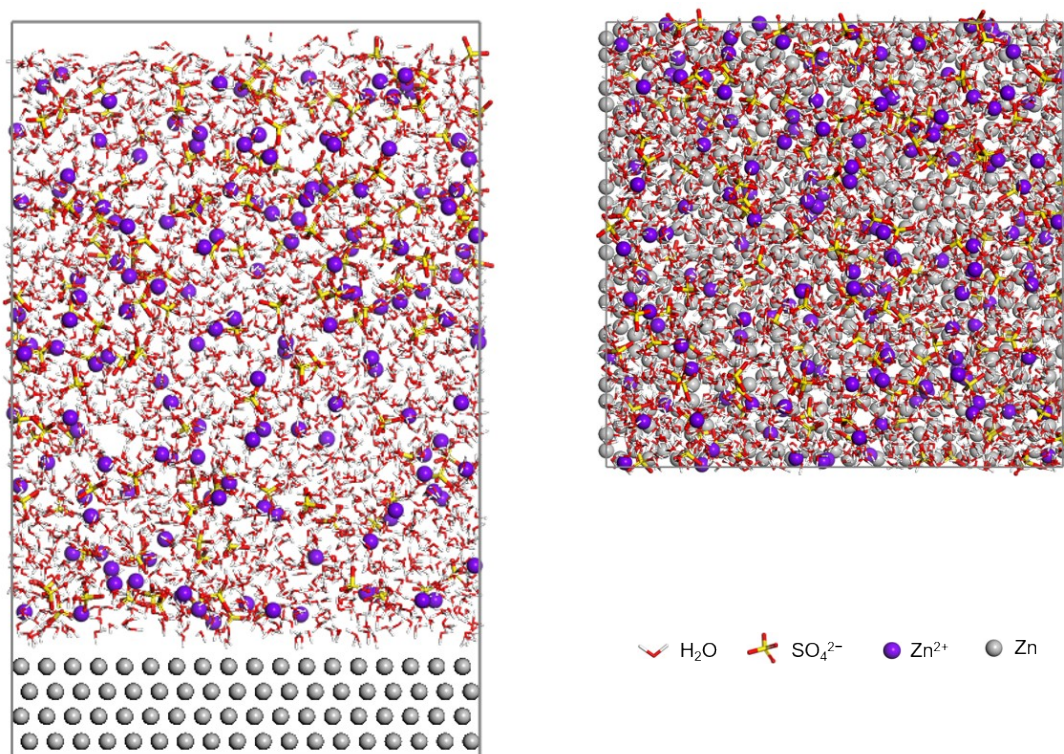


**Figure S12.** The visual simulation box of MD consisting of 3.0 M ZS electrolyte and a flat Zn electrode.

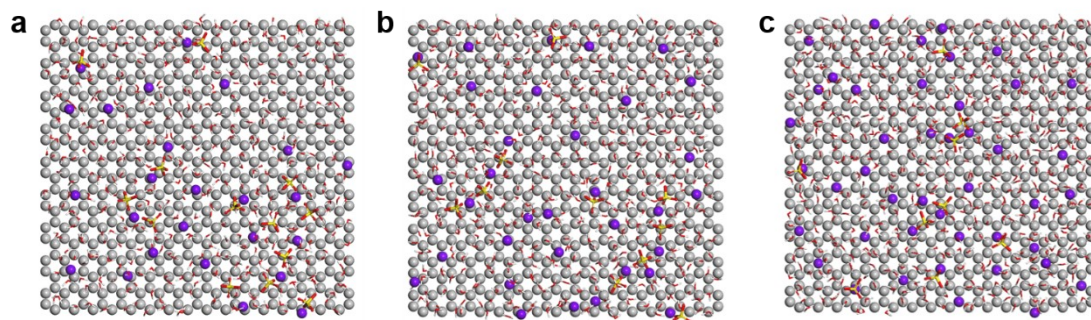


**Figure S13.** (a-c) Interfacial layering structures on Zn electrode surface using aqueous 3.0 M ZS electrolyte at (a)  $-0.13$ , (b)  $-0.23$ , and (c)  $-0.47$   $\text{C m}^{-2}$ .

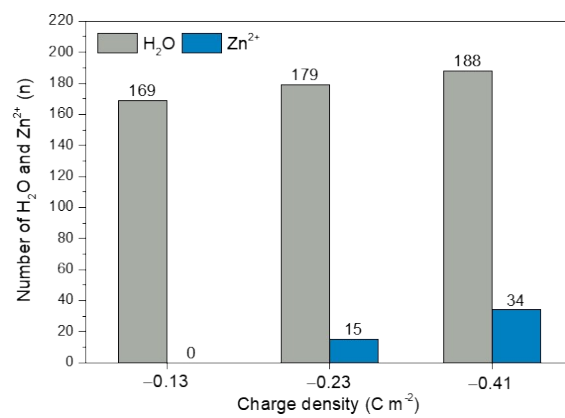


**Figure S14.** The numbers of H<sub>2</sub>O molecules and Zn<sup>2+</sup> ions in IHP at different negative charge densities of electrode surface.

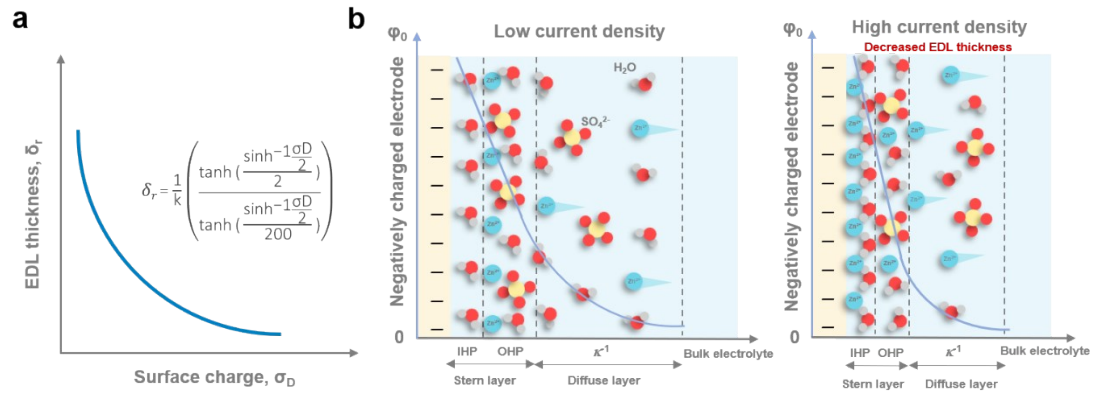


**Figure S15.** (a) EDL thickness versus surface charge density for Zn electrode. (b) Schematic illustration of the EDL structures at low and high current densities. The EDL thickness was reduced with the enhanced surface charge density based on the equation of  $\delta r$ , where  $k$  is invariable in the fixed ZS electrolyte and  $\sigma$  is surface charge density.

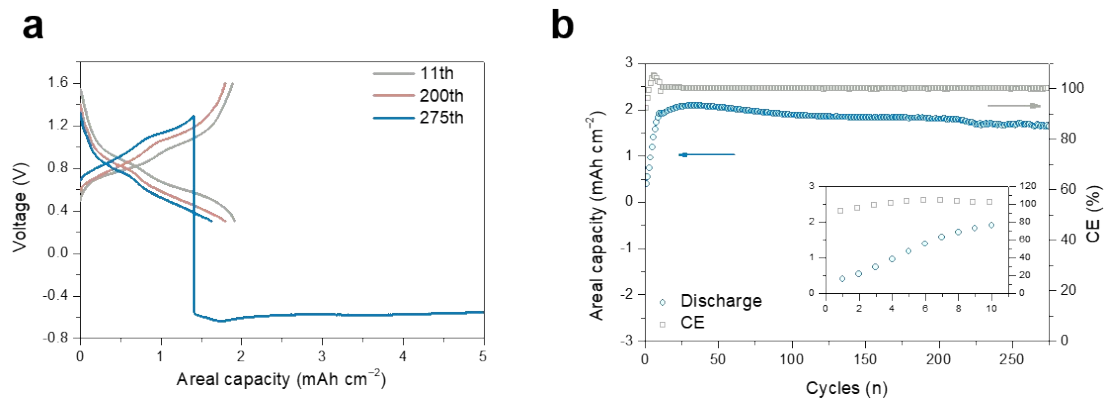


**Figure S16.** (a) The discharge/charge curves of Zn//V<sub>2</sub>O<sub>5</sub> battery at 4 mA cm<sup>-2</sup> and (b) the corresponding cycling stability. Insert: activation process at 1 mA cm<sup>-2</sup>.